



**HAL**  
open science

# Retrieval of upper tropospheric water vapor and upper tropospheric humidity from AMSU radiances

A. Houshangpour, V. O. John, S. A. Buehler

► **To cite this version:**

A. Houshangpour, V. O. John, S. A. Buehler. Retrieval of upper tropospheric water vapor and upper tropospheric humidity from AMSU radiances. *Atmospheric Chemistry and Physics*, 2005, 5 (8), pp.2019-2028. hal-00295710

**HAL Id: hal-00295710**

**<https://hal.science/hal-00295710>**

Submitted on 18 Jun 2008

**HAL** is a multi-disciplinary open access archive for the deposit and dissemination of scientific research documents, whether they are published or not. The documents may come from teaching and research institutions in France or abroad, or from public or private research centers.

L'archive ouverte pluridisciplinaire **HAL**, est destinée au dépôt et à la diffusion de documents scientifiques de niveau recherche, publiés ou non, émanant des établissements d'enseignement et de recherche français ou étrangers, des laboratoires publics ou privés.

# Retrieval of upper tropospheric water vapor and upper tropospheric humidity from AMSU radiances

A. Houshangpour, V. O. John, and S. A. Buehler

Institute of Environmental Physics, University of Bremen, Bremen, Germany

Received: 15 October 2004 – Published in Atmos. Chem. Phys. Discuss.: 15 March 2005

Revised: 15 June 2005 – Accepted: 14 July 2005 – Published: 5 August 2005

**Abstract.** A regression method was developed to retrieve upper tropospheric water vapor (UTWV in  $\text{kg/m}^2$ ) and upper tropospheric humidity (UTH in %RH) from radiances measured by the Advanced Microwave Sounding Unit (AMSU). In contrast to other UTH retrieval methods, UTH is defined as the average relative humidity between 500 and 200 hPa, not as a Jacobian weighted average, which has the advantage that the UTH altitude does not depend on the atmospheric conditions. The method uses AMSU channels 6–10, 18, and 19, and should achieve an accuracy of  $0.48 \text{ kg/m}^2$  for UTWV and  $6.3\% \text{ RH}$  for UTH, according to a test against an independent synthetic data set. This performance was confirmed for northern mid-latitudes by a comparison against radiosonde data from station Lindenberg in Germany, which yielded errors of  $0.23 \text{ kg/m}^2$  for UTWV and  $6.1\% \text{ RH}$  for UTH.

## 1 Introduction

Water vapor is the principal contributor to the greenhouse effect, as it absorbs and emits radiation across the entire longwave spectrum. Although water vapor in the upper troposphere represents a small fraction of the total vapor mass, it affects significantly the outgoing longwave radiation (Udelhofen and Hartmann, 1995; Schmetz et al., 1995; Spencer and Braswell, 1997; Held and Soden, 2000).

Several previous studies have demonstrated the feasibility of utilizing infrared satellite observations to retrieve upper tropospheric humidity. A simple radiance-to-UTH relationship was first derived by Soden and Bretherton (1993), indicating that the clear sky brightness temperature measured at a strong water vapor absorption line is proportional to the natural logarithm of the dividend of UTH over the cosine of the

satellite viewing angle. Their method provides a high computational speed in transforming brightness temperature to relative humidity by eliminating a full retrieval. Here, UTH is a Jacobian weighted mean of the fractional relative humidity in the upper troposphere. The Jacobian weighted definition of UTH has the disadvantage that the associated altitude range depends on the atmospheric condition and sensor characteristics. For moister atmospheres higher altitude ranges are sampled.

In contrast to the above approach, we define UTH as the mean relative humidity between 200 and 500 hPa to acquire a unique atmospheric parameter. An extended model is presented to retrieve UTH from AMSU radiances. This model makes use of upper tropospheric water vapor (UTWV), defined as the column integrated water vapor content between 200 and 500 hPa, and of upper tropospheric temperature information, which are both derived also from the AMSU measurements, so no external ancillary data is used. The method developed is a combination of regression techniques and a simple physical model of the observing system, one could call it a regression on a physical basis. In the derivation of the retrieval method some simplifying assumptions were made. These can be justified by the subsequent comparison of retrieved humidity parameters to radiosonde data.

## 2 AMSU data

The Advanced Microwave Sounding Unit (AMSU) consists of two instruments, AMSU-A and AMSU-B. The details on these instruments can be found in Mo (1996) and Saunders et al. (1995), respectively. They are cross-track scanning microwave sensors with a swath width of approximately 2300 km. These instruments measure microwave thermal emission emitted by the atmosphere in the oxygen band of 50–58 GHz (AMSU-A), the two water vapor lines at 22 GHz (AMSU-A) and 183 GHz (AMSU-B), and window regions

Correspondence to: A. Houshangpour  
(arash@sat.physik.uni-bremen.de)

(both). AMSU has 20 channels, where channels 1–15 belong to AMSU-A and channels 16–20 belong to AMSU-B. Temperature information of the atmosphere can be obtained from channels 4–14 of AMSU-A, where channels 6–8 give information on the upper troposphere. The three channels 18, 19, and 20 of AMSU-B which are centered around the 183.31 GHz water vapor line can give humidity information on the upper, middle, and lower troposphere, respectively.

AMSU-A and AMSU-B scan the atmosphere with different footprints. AMSU-A samples the atmosphere in 30 scan positions across the track with a footprint size of  $50 \times 50 \text{ km}^2$  for the innermost scan position. This size increases to  $150 \times 80 \text{ km}^2$  for the outermost position scan position. AMSU-B samples the atmosphere in 90 scan positions with footprint size varying from  $20 \times 16 \text{ km}^2$  to  $64 \times 27 \text{ km}^2$ .

### 3 UTWV methodology

To derive a basic radiance to UTWV relationship, attention will be focused on a model atmosphere in which the water vapor density  $\rho_{H_2O}$  decreases exponentially with altitude,

$$\rho_{H_2O}(z) = \rho_0 \exp\left\{-\frac{z}{H}\right\}, \quad (1)$$

and the tropospheric temperature lapse rate  $\beta$  is constant,

$$T(z) = \beta z + T_0. \quad (2)$$

According to Eq. (1) the total mass of water vapor contained in a vertical column of unit cross section ranging from a given level  $z^*$  to the top of the atmosphere is given by

$$wv(z^*) = \int_{z^*}^{\infty} \rho_{H_2O}(z) dz = \rho_0 H \exp\left\{-\frac{z^*}{H}\right\}, \quad (3)$$

where the scale height  $H$  is considered constant. Hence, the task will be to derive the required parameter  $\rho_0$  from water vapor channel radiances.

Assuming the absorption coefficient  $\alpha$  associated with the water vapor channel of concern is proportional to  $\rho_{H_2O}$ ,

$$\alpha(z) = F \rho_{H_2O}(z), \quad (4)$$

where  $F$  is a channel specific constant, it can be shown (Elachi, 1987) that the peak of the channel weighting function is located at the altitude

$$z_P = H \ln\{F \rho_0 H\}. \quad (5)$$

Except for extremely dry profiles, AMSU-B channel 18 and 19 exhibit bell-shaped weighting functions, being approximately symmetric in the region centered around the peak value, namely the atmospheric layer with the highest contribution to the observed brightness temperature. Since temperature is assumed to be linearly dependent on altitude, its weighting with a symmetric function in the region of concern yields the atmospheric temperature at the level  $z_P$ , thus the corresponding brightness temperature is

$$T_B = T(z_P) = \beta z_P + T_0. \quad (6)$$

Substituting  $z_P$  and solving for  $\rho_0$  yield:

$$\rho_0 = \frac{1}{FH} \exp\left\{\frac{1}{\beta H}(T_B - T_0)\right\}. \quad (7)$$

Inserting the above expression in Eq. (3), upper tropospheric water vapor is given by

$$\begin{aligned} UTWV &= wv(T_B, \beta, T_0; z^*) \\ &= \frac{1}{F} \exp\left\{-\left(\frac{z^*}{H} + \frac{T_0}{\beta H}\right)\right\} \exp\left\{\frac{T_B}{\beta H}\right\}, \end{aligned} \quad (8)$$

where  $z^*$  is now set to the 500 hPa level and the amount of water vapor above 200 hPa is neglected. The model presented above is used in this study to retrieve UTWV from AMSU water vapor channel radiances. To this end first a scaling approach is applied to eliminate the explicit temperature dependence of UTWV, which is then fitted exponentially to obtain the desired model parameters.

#### 3.1 Scaling approach

Given the water vapor and temperature profile of an atmospheric situation along with the corresponding brightness temperature, the aim of the scaling approach is to determine the brightness temperature that is measured assuming that only the temperature profile changes.

By this means it will be possible to set the temperature parameters  $\beta$  and  $T_0$  in Eq. (8) to fixed values and transform the brightness temperature  $T_B$  in such a way that UTWV is preserved.

To illustrate the scaling approach, consider a sufficiently moist atmospheric situation for which the ground contribution to the radiance measured at the water vapor channel of concern might be neglected, so the corresponding brightness temperature is given by

$$T_B = \int_{z_1}^{z_2} WF(z) T(z) dz, \quad (9)$$

where  $WF(z)$  is the channel weighting function ranging from  $z_1$  to  $z_2$  and  $T(z)$  is the temperature being a linear function of altitude over the range  $[z_1, z_2]$ . Now suppose  $T(z)$  in Eq. (9) is replaced by a new temperature profile  $T^*(z)$  given by the parameters  $\beta^*$  and  $T_0^*$ :

$$T^*(z) = \beta^* z + T_0^*, \quad (10)$$

thus the resulting brightness temperature is given by

$$T_B^* = \int_{z_1}^{z_2} WF^*(z) T^*(z) dz. \quad (11)$$

A further assumption made is, that when evaluating the integral in Eq. (11), the temperature dependence of the weighting function is negligible compared to the variation of  $T(z)$  itself,

$$WF^*(z) \approx WF(z). \quad (12)$$

From Eqs. (2) and (10),  $T^*(z)$  can be written as a function of  $T(z)$ :

$$T^*(z) = \frac{\beta^*}{\beta} (T(z) - T_0) + T_0^*. \quad (13)$$

Substituting  $T^*(z)$  in Eq. (11) and using the approximation in Eq. (12), the transformed brightness temperature is given by

$$T_B^* = \int_{z_1}^{z_2} WF(z) \left\{ \frac{\beta^*}{\beta} (T(z) - T_0) + T_0^* \right\} dz \quad (14)$$

$$\begin{aligned} &= \frac{\beta^*}{\beta} \int_{z_1}^{z_2} WF(z) T(z) dz - T_0 \frac{\beta^*}{\beta} \int_{z_1}^{z_2} WF(z) dz \\ &+ T_0^* \int_{z_1}^{z_2} WF(z) dz. \end{aligned} \quad (15)$$

The integral in the first term of Eq. (15) is the initial brightness temperature as given in Eq. (9) and the integral appearing in the second and third term can be set to unity, as the weighting function is assumed to be normalized over the altitude range  $[z_1, z_2]$ , thus the final expression found for  $T_B^*$  is

$$T_B^* = \frac{\beta^*}{\beta} T_B + T_0^* - T_0 \frac{\beta^*}{\beta}. \quad (16)$$

Replacing  $T_B$ ,  $\beta$  and  $T_0$  in Eq. (8) by  $T_B^*$ ,  $\beta^*$  and  $T_0^*$  respectively, and taking logs, upper tropospheric water vapor is given by

$$\ln(UTWV(T_B^*)) = \ln C_0 + C_1 T_B^*, \quad (17)$$

where

$$C_0 = \frac{1}{F} \exp \left\{ - \left( \frac{z^*}{H} + \frac{T_0^*}{\beta^* H} \right) \right\} \quad (18)$$

$$C_1 = \frac{1}{\beta^* H}. \quad (19)$$

The fitting procedure of  $\ln UTWV$  will be demonstrated on the basis of ECMWF-data in Sect. 5. The estimation of the temperature parameters  $\beta$  and  $T_0$  required to perform the linear transformation in Eq. (16) is the objective of the following section.

### 3.2 Temperature parameters

AMSU-A temperature channels 6–10 are used to estimate the parameters  $\beta$  and  $T_0$ . Figure 1 shows the weighting functions at the AMSU-A innermost viewing angle of  $1.65^\circ$  for a model profile from the ECMWF analysis along with the corresponding temperature profile. Approximating the atmospheric temperature by

$$T(z) = \beta z + T_0 \quad (z < z_{TP}) \quad (20)$$

$$T(z) = T_{TP} \quad (z_{TP} \leq z < z_{ST}) \quad (21)$$

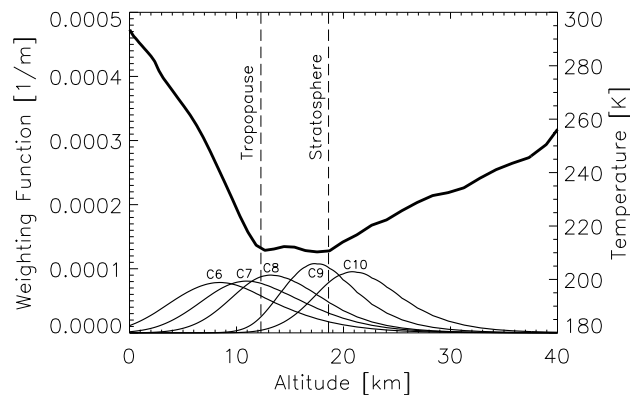


**Fig. 1.** ARTS simulated AMSU-A channel 6–10 weighting functions at near-nadir for a model atmosphere from the ECMWF analysis along with the corresponding temperature profile.

$$T(z) = \gamma(z - z_{ST}) + T_{TP} \quad (z \geq z_{ST}), \quad (22)$$

where  $T_{TP}$  is the tropopause temperature,  $z_{TP}$  and  $z_{ST}$  denote the lower boundary heights of the tropopause and the stratosphere respectively and  $\gamma$  represents the stratospheric lapse rate, the brightness temperatures observed by the sensor can be written as

$$\begin{aligned} T_i &= S_i + \int_{z_S}^{z_{TP}} WF_i(z) (\beta z + T_0) dz \\ &+ \int_{z_{TP}}^{z_{ST}} WF_i(z) T_{TP} dz \\ &+ \int_{z_{ST}}^{\infty} WF_i(z) (\gamma(z - z_{ST}) + T_{TP}) dz. \end{aligned} \quad (23)$$

where  $i$  denotes the channel number ( $i=6, \dots, 10$ ),  $WF$  is the weighting function,  $S$  is the surface contribution to the observed brightness temperature, and  $z_S$  is the surface height. Replacing  $T_{TP}$  by  $\beta z_{TP} + T_0$ , rearranging, and using the normalization of  $WF(z)$  yield

$$T_i = S_i + T_0 + Q_i \beta + R_i \gamma \quad (i = 6, \dots, 10). \quad (24)$$

where

$$Q_i = \int_{z_S}^{z_{TP}} WF_i(z) z dz + \int_{z_{TP}}^{\infty} WF_i(z) z_{TP} dz \quad (25)$$

$$R_i = \int_{z_{ST}}^{\infty} WF_i(z) (z - z_{ST}) dz \quad (26)$$

From Eq. (24), the parameters  $T_0$ ,  $\beta$ , (and  $\gamma$ ) can be expressed as linear combinations of the brightness temperatures  $T_i$

$$T_0 = C_{T_0,0} + \sum_{i=6}^{10} C_{T_0,i} T_i \quad (27)$$

$$\beta = C_{\beta,0} + \sum_{i=6}^{10} C_{\beta,i} T_i. \quad (28)$$

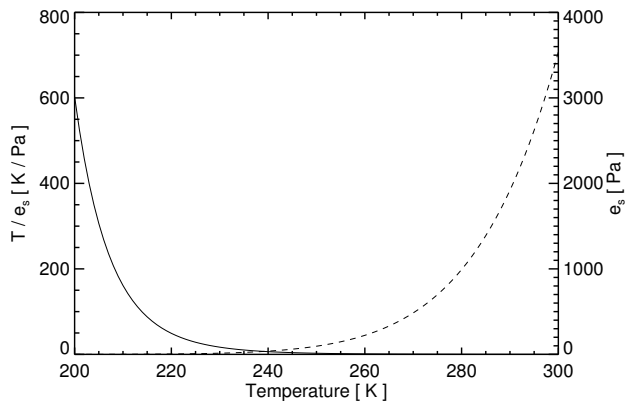


**Fig. 2.** Variations with temperature of the saturation water vapor pressure  $e_s$  (dashed) and of temperature divided by saturation water vapor pressure  $\frac{T}{e_s(T)}$  (solid). In both cases  $e_s$  is with respect to liquid water.

The quantities  $C_{T_0,i}$  and  $C_{\beta,i}$  are functions of surface height, temperature, and emissivity ( $S_i$ ) as well as  $z_{TP}$  and  $z_{ST}$ . Nevertheless they will be regarded as constants to enable their estimation by multiple linear regression. Hence the regression coefficients obtained in this way will be weighted means according to the statistics of the data set used.

The validation of the methodology developed above is postponed to Sects. 5 and 6. Assuming knowledge of  $T_0$ ,  $\beta$  and UTWV, we proceed to derive upper tropospheric humidity from water vapor channel radiances.

#### 4 UTH methodology

One could be tempted to calculate UTH directly from the retrieved UTWV and mean upper tropospheric temperature. However, the attempt fails because the combined errors in temperature and particularly UTWV lead to a large error in UTH. Instead, our approach is as follows: the relative humidity profile of a model atmosphere as specified in the previous section is given by

$$\frac{RH(z)}{100} = \frac{e(z)}{e_s(z)} \quad (29)$$

$$= R_v \frac{UTWV}{H} \exp\left\{\frac{z^* - z}{H}\right\} \frac{T(z)}{e_s(T(z))}, \quad (30)$$

where  $e$  is the actual water vapor pressure,  $e_s$  is the saturation vapor pressure with respect to water, and  $R_v$  is the gas constant for 1 kg of water vapor. As Fig. 2 indicates, the term  $\frac{T}{e_s(T)}$  shows an exponential behavior in the tropospheric temperature range. Thus the relative humidity profile given by Eq. (30) may be approximated by an exponential function of altitude, as  $T$  and  $z$  are linearly dependent variables. Assuming that the mean upper tropospheric humidity is equivalent

to the relative humidity at a fixed level  $z_0$  in the upper troposphere

$$UTH = RH(z_0), \quad (31)$$

UTH can be derived using two appropriate profile points, namely the ones provided by AMSU water vapor channels 18 and 19. The relative humidities at the associated peak levels  $z_{18}$  and  $z_{19}$  are

$$RH_i = R_v \frac{UTWV}{H} \exp\left\{\frac{z^*}{H}\right\} \exp\left\{\frac{T_0 - T_i}{\beta H}\right\} \times \frac{T_i}{e_s(T_i)} \quad (i = 18, 19). \quad (32)$$

The given profile points ( $z_{18}$ ,  $RH_{18}$ ) and ( $z_{19}$ ,  $RH_{19}$ ) can be used to estimate the UTH equivalent value  $RH(z_0)$ . Linearizing by taking logs, and considering  $z_{18} - z_{19}$  as constant according to Eq. (5), we get

$$\begin{aligned} \ln UTH &= K_0 + K_1(\ln UTWV) \\ &+ K_2\left(\frac{T_0 - T_{18}}{\beta}\right) \\ &+ K_3(\ln T_{18}) \\ &+ K_4(\ln e_{s,18}) \\ &+ K_5\left(\frac{T_0 - T_{19}}{\beta}\right) \\ &+ K_6(\ln T_{19}) \\ &+ K_7(\ln e_{s,19}) \\ &+ K_8\left(\frac{T_0 - T_{18}}{\beta} \ln UTWV\right) \\ &+ K_9(\ln T_{18} \ln UTWV) \\ &+ K_{10}(\ln e_{s,18} \ln UTWV) \\ &+ K_{11}\left(\frac{T_0 - T_{19}}{\beta} \ln UTWV\right) \\ &+ K_{12}(\ln T_{19} \ln UTWV) \\ &+ K_{13}(\ln e_{s,19} \ln UTWV). \end{aligned} \quad (33)$$

As will be shown in Sect. 5, the above fit provides an excellent UTH retrieval if involving true  $T_0$ -,  $\beta$ - and UTWV-values. However Eq. (33) turns out to be sensitive to retrieval errors associated with  $\beta$  and UTWV. The  $\beta$ -sensitivity will be treated by defining a criterion to exclude inappropriate  $\beta$ -values. To reduce the sensitivity to UTWV, the water vapor information is utilized in a parametric manner by performing the fit on specific UTWV groups. In this way we obtain different fit parameters according to different groups. Considering UTWV to be fixed in each group, Eq. (33) will be reduced as follows:

$$\begin{aligned} \ln UTH &= L_0 + L_1\left(\frac{T_0 - T_{18}}{\beta}\right) \\ &+ L_2(\ln T_{18}) \\ &+ L_3(\ln e_{s,18}) \end{aligned}$$

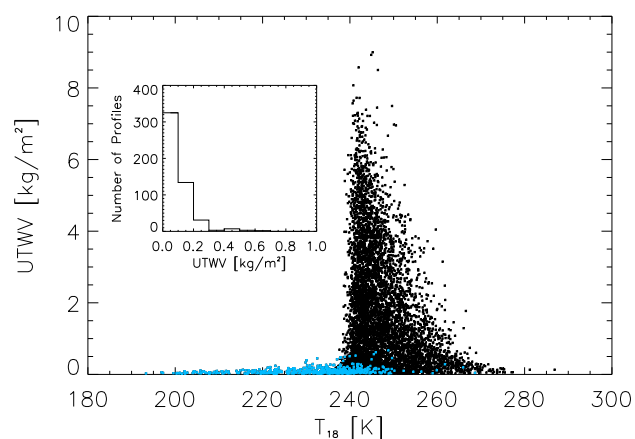


**Fig. 3.** Scatter plot of upper tropospheric water vapor content versus corresponding forward calculated AMSU-B channel 18 brightness temperature for the ECMWF training set. Blue indicates atmospheric situations specified by  $T_{19} \leq T_{18}$ . The inserted histogram gives the distribution of the outliers over upper tropospheric water vapor.

$$\begin{aligned}
 &+ L_4 \left( \frac{T_0 - T_{19}}{\beta} \right) \\
 &+ L_5 (\ln T_{19}) \\
 &+ L_6 (\ln e_{s,19})
 \end{aligned} \quad (34)$$

This linear model represents the basis of the UTH retrieval accomplished in this study. Alternatively, UTH could also be retrieved with only channel 18 at the cost of reducing the global accuracy. Channel 19 provides additional information, in particular for moist profiles.

## 5 Implementation of the algorithm

Model parameters for the retrieval algorithm presented above were derived on a global scale using the 60-level sampled database from the European Centre for Medium-Range Weather Forecasts (ECMWF) analysis (Chevallier, 2001). The ECMWF data set is a diverse set of 13 495 profiles designed to capture a wide range of atmospheric variability desired to perform statistical regressions or to validate an algorithm. The profiles were divided into two randomly drawn sets: a training set for deriving the model parameters, and a test set. For each profile upper tropospheric water vapor (UTWV) and upper tropospheric humidity (UTH) were determined. AMSU channel 6–10, 18, and 19 brightness temperatures were simulated at the sensor viewing angles associated with AMSU-A scan positions using ARTS 1.0 (Buehler et al., 2005) for cloud-free conditions and a surface emissivity of 0.9. In order to make the synthetic radiances realistic, instrument specific noise was added. The true temperature parameters  $\beta$  and  $T_0$  were derived by linearly fitting the temperature versus altitude in the pressure range 200–500 hPa.

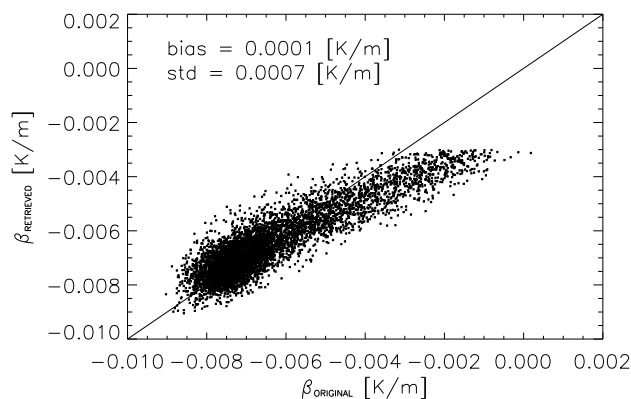


**Fig. 4.** Scatter plot of retrieved versus original upper tropospheric temperature lapse rate  $\beta$  for the ECMWF test set. Bias and absolute error are indicated.

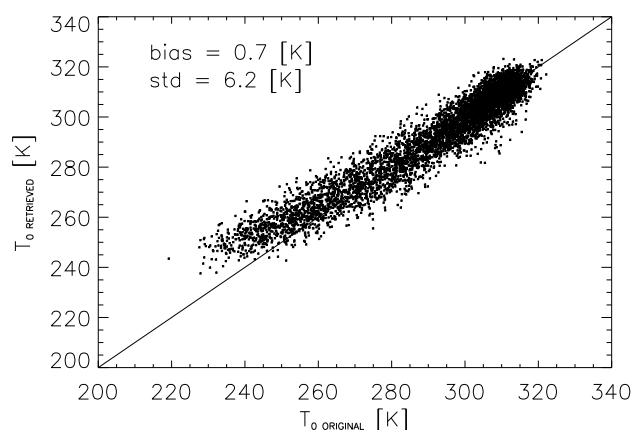


**Fig. 5.** As Fig. 4 but for the upper tropospheric temperature offset  $T_0$ .

Since the retrieval approach is identical for all viewing angles, its description will be restricted to the AMSU-A innermost viewing angle of  $1.65^\circ$ . Figure 3 shows the scatter plot of UTWV versus corresponding  $T_{18}$  for the training set. In relating water vapor channel radiances to UTWV, outliers are primarily expected to occur in very dry atmospheric situations, when the weighting function exhibits a (near)-surface peak making the brightness temperature mainly dependent on surface temperature and emissivity. Such dry cases principally originate in polar or high elevated regions, thus possessing a low surface temperature. As AMSU-B channel 19 generally peaks lower than AMSU-B channel 18, the criterion  $T_{19} \leq T_{18}$  can be used to identify and exclude the outliers mentioned above (see Fig. 3). Figure 3 also shows the distribution of the discarded profiles over UTWV. Obviously the condition  $T_{19} \leq T_{18}$  already allows a good estimation of the respective UTWV values, being lower than  $0.3 \text{ kg/m}^2$ . A further criterion to exclude outliers pertains to the (upper) tropospheric lapse rate  $\beta$  due to its involvement in the

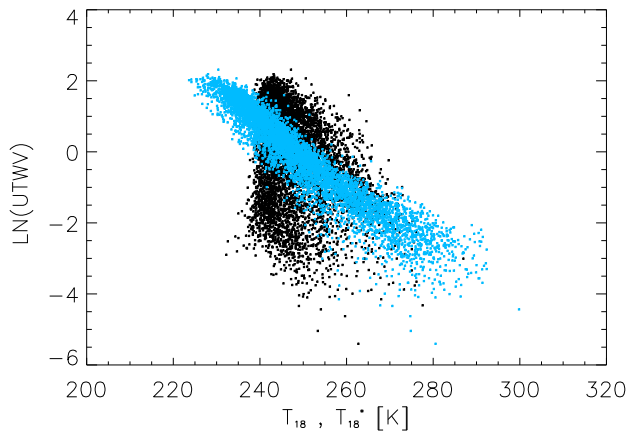


**Fig. 6.** Scatter plot of the natural logarithm of upper tropospheric water vapor versus corresponding: (black) AMSU-B channel 18 brightness temperature, and (blue) transformed AMSU-B channel 18 brightness temperature.

transformation (16). Since the variables  $T_0$  and  $\beta$  in Eq. (16) represent an approximation of the true tropospheric temperature profile, the scaled brightness temperature  $T_B^*$  will be associated with an error, which may be given by

$$\Delta T_B^* = \left| \frac{\beta^*}{\beta^2} (T_0 - T_B) \right| \Delta \beta + \left| -\frac{\beta^*}{\beta} \right| \Delta T_0. \quad (35)$$

From Eq. (35),  $\Delta T_B^*$  diverges as  $\beta$  tends towards zero. The calculated lapse rates for the ECMWF data set lie in the range from  $-0.01$  to  $0.002$  K/m. Profiles with  $\beta \geq -0.003$  K/m were excluded. This criterion also excludes  $\beta$ -values critical to the UTH model given by Eq. (34). The training set was obtained by utilizing the criteria specified above. The regression coefficients  $C_{T_0,i}$  and  $C_{\beta,i}$  required to provide tropospheric temperature information via Eqs. (27) and (28) were estimated by performing a multiple linear regression fit. Figures 4 and 5 compare  $\beta$ - and  $T_0$ -values retrieved by applying the linear models (27) and (28) to the test set with the corresponding original values.

To retrieve upper tropospheric water vapor according to Eq. (17), the temperature parameters  $\beta$  and  $T_0$  were utilized to transform AMSU-B channel 18 and 19 brightness temperatures via Eq. (16) to a reference temperature profile  $T^*(z) = \beta^* z + T_0^*$ , where  $\beta^*$  and  $T_0^*$  were set to the mean values obtained from the ECMWF data set, namely  $\beta^* = -0.006$  K/m and  $T_0^* = 290$  K. It turned out that the retrieval results are not sensitive to the choice of the reference temperature profile. Figures 6 and 7 illustrate how the shape of the scatter plots of  $\ln(\text{UTWV})$  versus  $T_{18}$  and  $T_{19}$  is modified due to the scaling approach. The performance of the linear fit given by Eq. (17) was facilitated by the fact that the information content of the radiance detected by a sensor sounding an irregular atmosphere is limited to integrated quantities over the range of its weighting function.

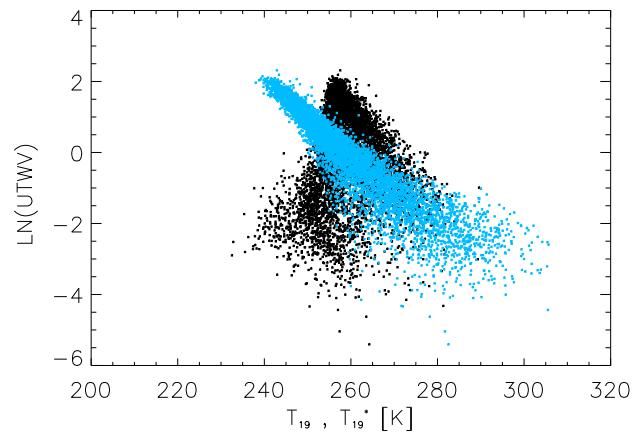


**Fig. 7.** As Fig. 6 but for AMSU-B channel 19.

Due to stronger water vapor absorption, as mentioned before, AMSU channel 18 peaks generally higher than channel 19, thus offering a larger coverage of the upper troposphere in low-UTWV cases. On the other hand, an increase in UTWV is associated with an upward shift of the water vapor channel weighting functions under consideration, making channel 19 appropriate in high-UTWV cases. Hence it is convenient to split the data set according to UTWV. This was accomplished by defining a cutoff value for  $T_{18}^*$ , denoted by  $T_{cut}$ .  $T_{cut}$  was set to 247 K, an optimal value determined empirically and fixed for all viewing angles. Data points given by  $T_{18}^* < T_{cut}$  were fitted using  $T_{19}^*$ , whereas  $T_{18}^*$  was used to fit the remaining subset. Figures 8 and 9 show the subsets along with the corresponding best-fit lines. The negative logarithmic slope here indicates that the expected retrieval error increases towards higher UTWV values. Figure 10 shows the scatter plot of retrieved versus original UTWV for the test set. The absolute error of UTWV retrieval is  $0.48$  kg/m<sup>2</sup>, the bias is  $-0.01$  kg/m<sup>2</sup>.

Before proceeding with the UTWV-parametric retrieval of upper tropospheric humidity according to the reduced model (34), we verify the full model (33), in which upper tropospheric water vapor is an explicit independent variable. To this end radiometric noise is omitted,  $T_0$ -,  $\beta$ - ,and UTWV-values are set to true, and Eq. (33) is applied considering  $T_{cut}$ . The excellent retrieval in the case of moist profiles, that is  $T_{18}^* < T_{cut}$  (see Fig. 11), confirms the UTH full model developed in Sect. 4. In the case of dry profiles, that is  $T_{18}^* \geq T_{cut}$  (see Fig. 12), the retrieval suffers from the fact that the water vapor channels peak lower in the troposphere and do not allow for an appropriate estimation of UTH. It should be noted that a high (*low*) value of the transformed brightness temperature  $T_{18}^*$  is not necessarily associated with a dry (*moist*) atmosphere, since  $T_{18}^*$  also depends on the temperature. To carry out the UTH retrieval on the basis of the reduced model (33), the data set was divided into sub-groups with respect to upper tropospheric water vapor content. The bin size was

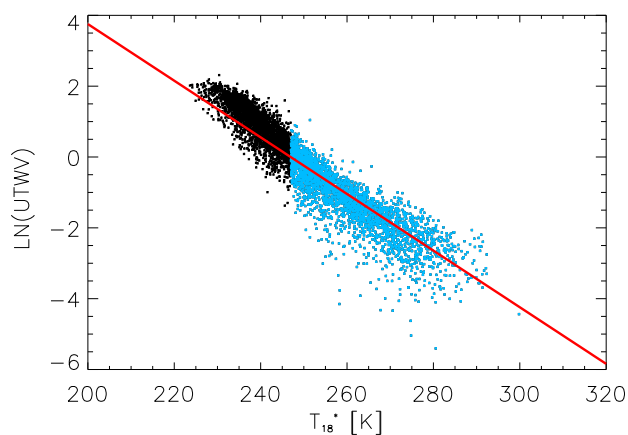


**Fig. 8.** Scatter plot of the natural logarithm of upper tropospheric water vapor versus corresponding transformed AMSU-B channel 18 brightness temperature along with the best-fit straight line (red) to the subset specified by  $T_{18}^* \geq 247$  K.

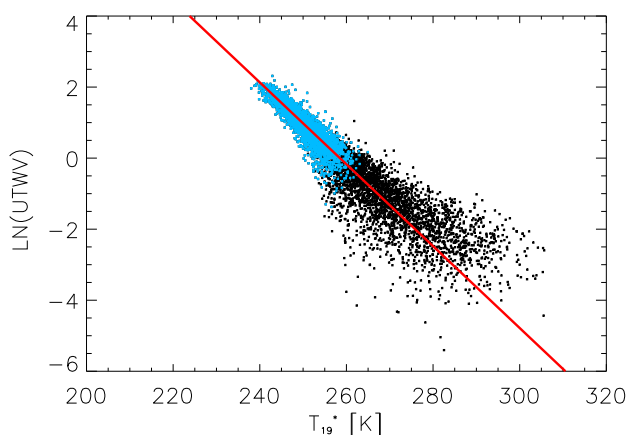


**Fig. 9.** Scatter plot of the natural logarithm of upper tropospheric water vapor versus corresponding transformed AMSU-B channel 19 brightness temperature along with the best-fit straight line (red) to the subset specified by  $T_{18}^* < 247$  K.

chosen to be  $1 \text{ kg/m}^2$ , except for the first sub-group ranging from 0 to  $0.5 \text{ kg/m}^2$ . Model parameters  $L_i$  were determined by performing a multiple linear regression on the test set. The UTH retrieval results are given in Fig. 13. The observed negative bias arises primarily from an overestimation of upper tropospheric temperature. In addition, the number of profiles used in the case of high UTWV sub-groups may be insufficient to provide the statistical basis to determine the desired fit coefficients. However the overall absolute error of the UTH retrieval for the ECMWF data set is  $6.3\% RH$ , the bias is  $-0.5\% RH$ .

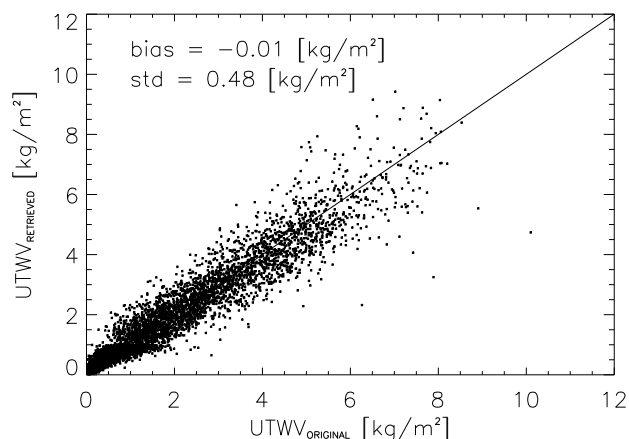


**Fig. 10.** Scatter plot of retrieved versus original upper tropospheric water vapor content UTWV for the ECMWF test set. Bias and absolute error are indicated.

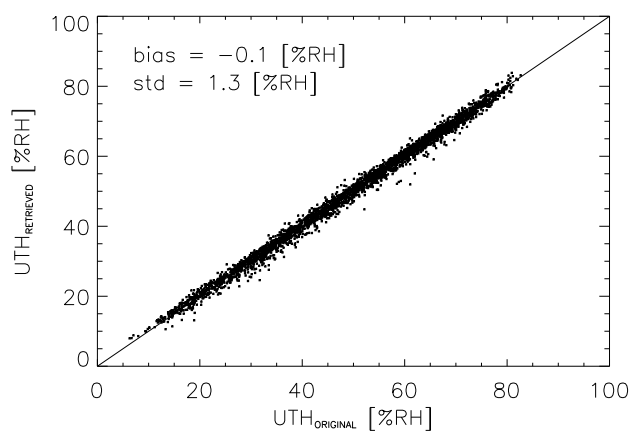


**Fig. 11.** Scatter plot of upper tropospheric humidity retrieved using the full model (33) versus corresponding original values for ECMWF test profiles given by  $T_{18}^* < 247$  K. Bias and absolute error are indicated. Note that here the true values of the required model variables have been used, with the aim to verify the model formulation.

## 6 Validation

In order to validate the algorithm, we used two years (November 2001–October 2003) of co-located AMSU and radiosonde data. The radiosonde data is from Lindenberg ( $52^\circ 22' \text{ N}$ ,  $14^\circ 12' \text{ E}$ ), which is a reference station of the German weather service. The data from this station have been undergone several quality control measures and corrections (Leiterer et al., 1997). The procedure of collocation is described in detail in Buehler et al. (2004), henceforth referred to as BKJ.

Apart from the filters used in BKJ, there are two more filters used here. One filter is related to the inhomogeneity of the atmosphere represented by the standard deviation of

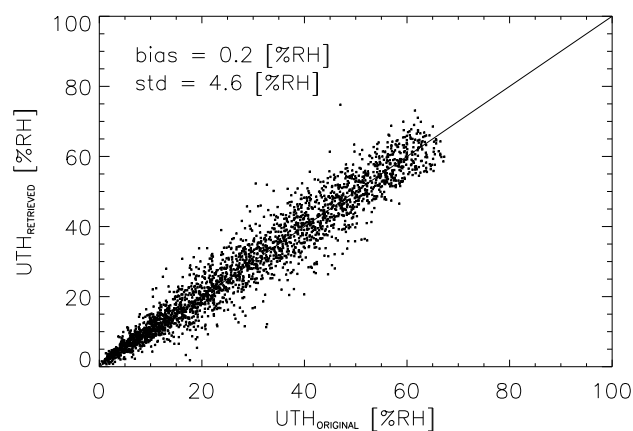


**Fig. 12.** As Fig. 11 but for ECMWF test profiles given by  $T_{18}^* \geq 247$  K.

brightness temperature in a circle of 50 km radius around the station ( $\sigma_{50\text{km}}$ ). In BKJ, none of the matches were discarded based on the value of  $\sigma_{50\text{km}}$ , instead, an error model was developed considering the  $\sigma_{50\text{km}}$ . In the present validation procedure, instead of using the error model, we discarded the matches which have  $\sigma_{50\text{km}}$  for channel 18 of AMSU greater than 1.5 K. This filter ensures that the matches we used to validate the algorithm are homogeneous cases.

Another filter is related to the upper tropospheric lapse rate ( $\beta$ ) retrieved from the temperature channels of AMSU. The matches with the lapse rate greater than or equal to  $-0.003$  K/m are discarded, which is part of the algorithm and is explained in Sect. 5.

UTH, UTWV,  $T_0$ , and  $\beta$  were computed from the radiosonde profiles by interpolating the humidity and temperature profiles on to a fine pressure grid extending from 500 hPa to 200 hPa. Figure 14 shows the agreement between the UTWV computed from radiosonde data ( $UTWV_{\text{SONDE}}$ ) and the UTWV retrieved from AMSU data ( $UTWV_{\text{AMSU}}$ ). Though the bias is approximately zero there exists a slope, i.e. higher UTWV values are underestimated. The absolute error of UTWV retrieval is  $0.23$  kg/m<sup>2</sup>. UTH retrieval also shows good agreement with radiosonde UTH (see Fig. 15). The bias is  $0.4\%$  RH and the retrieval error  $6.1\%$  RH. These values are consistent with the values given by Jimenez et al. (2004) and Buehler and John (2005).

There exists a non-unity slope in the case of UTH also which appears to be due to the underestimation at very low UTH-values by radiosondes (Buehler et al., 2004). A validation with radiosonde data from other stations would be desirable and is planned as a future activity. The problem here is to find radiosonde data of sufficiently high quality which is particularly deficient for the tropical stations.

## 7 Conclusions

A physically based regression method to derive upper tropospheric humidity (UTH) from AMSU radiances was presented. The logarithm of UTH was shown to be given by a linear model in which the regressors are functions of AMSU-B channel 18 and 19 brightness temperatures, upper tropospheric water vapor (UTWV), and upper tropospheric temperature parameters.

Assuming a model atmosphere, upper tropospheric temperature parameters could be approximated by linear combinations of AMSU-A temperature channel radiances (AMSU-A channels 6–10).

The retrieval of upper tropospheric water vapor was facilitated by transforming the corresponding water vapor channel radiances (AMSU-B channels 18 and 19) to a fixed atmospheric temperature profile using upper tropospheric temperature information. It was shown that UTWV is then an exponential function of the transformed brightness temperature under consideration. This exponential relationship could be easily linearized by taking logs.

The original UTH model incorporating upper tropospheric water vapor as an explicit variable provides an excellent UTH retrieval when involving true values. However, it turned out to be sensitive to UTWV retrieval errors. To reduce this sensitivity, upper tropospheric water vapor information was utilized in a parametric manner by considering the model on fixed UTWV groups.

Coefficients required to accomplish the retrievals according to the linear models developed in this study were determined by multiple linear regression on a global scale using the 60-level sampled database from the ECMWF analysis. The theoretical retrieval accuracy was estimated on the basis of an independent set of synthetic data. Absolute retrieval errors of UTWV and UTH are  $0.48$  kg/m<sup>2</sup> and  $6.3\%$  RH, respectively. In order to validate the algorithm, two years (November 2001–October 2003) of co-located AMSU and radiosonde data from Lindenberg (Germany) were used. The absolute error of the UTWV retrieval was  $0.23$  kg/m<sup>2</sup>. The higher accuracy here arises from the fact that the UTWV retrieval error decreases towards drier upper tropospheric conditions. The UTH absolute error was  $6.1\%$  RH. This value is consistent with the result obtained from the synthetic data.

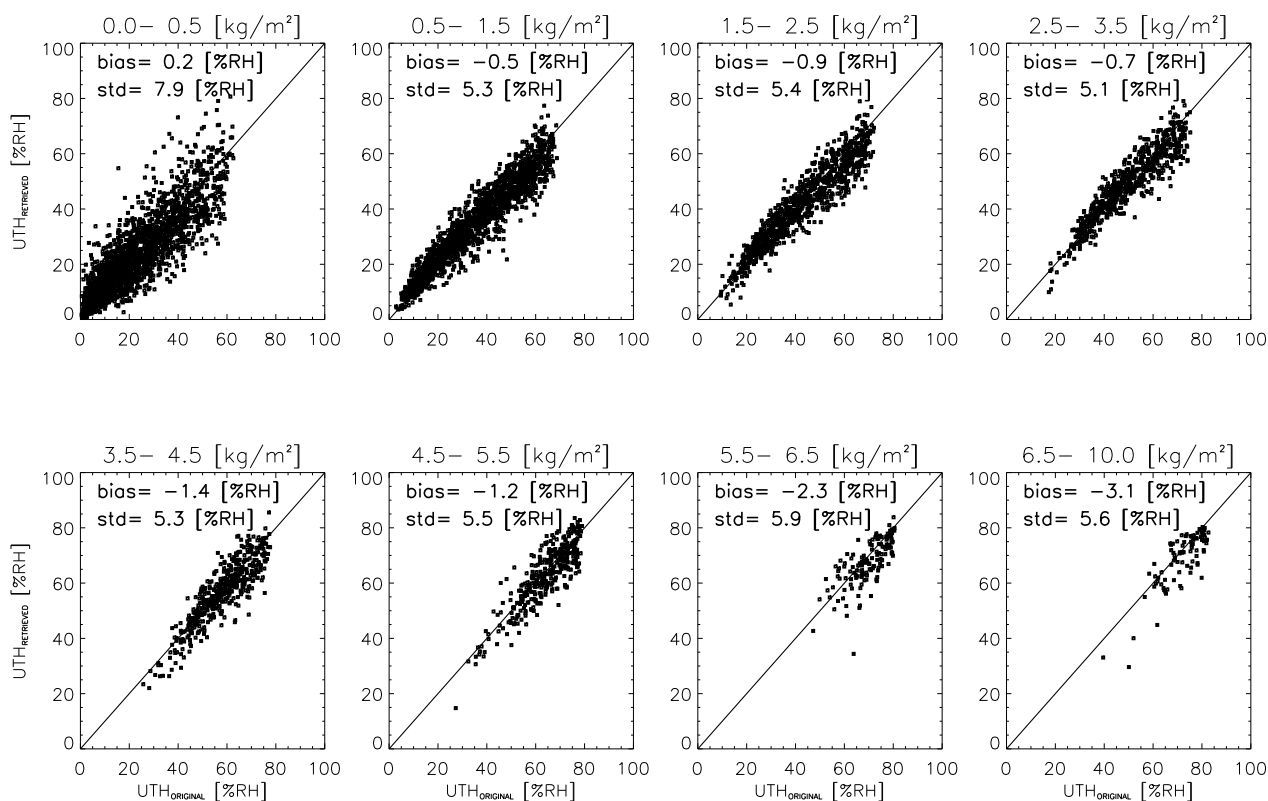


**Fig. 13.** Scatter plot of upper tropospheric humidity retrieved using the reduced model (34) versus corresponding original values for the ECMWF test set. The plotting titles indicate the respective UTWV groups. Biases and absolute errors are indicated.

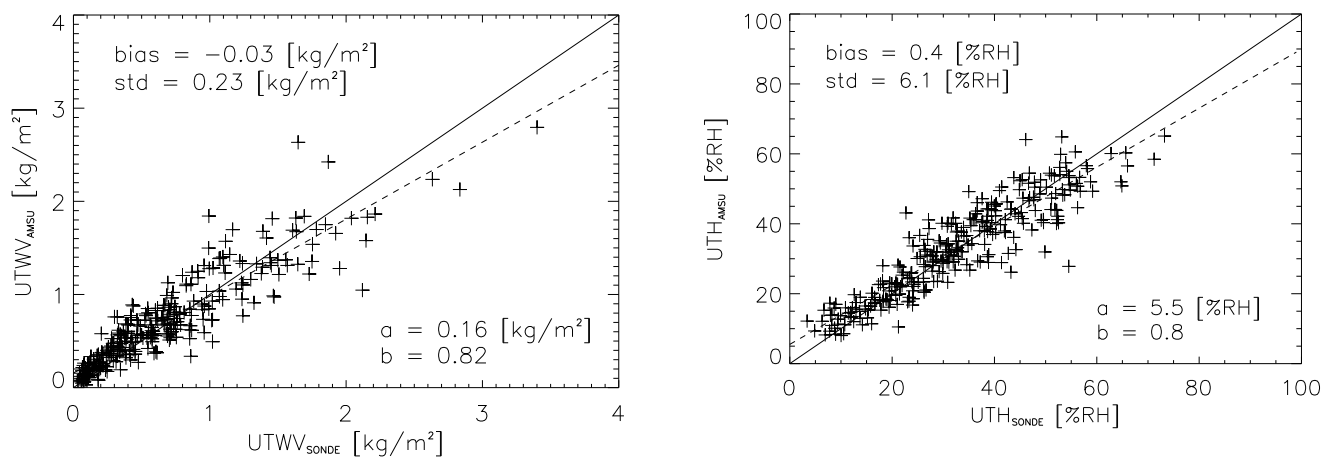


**Fig. 14.** Comparison of upper tropospheric water vapor content derived from co-located AMSU and radiosonde measurements near Lindenberg (Germany) in the time between November 2001 and October 2003. Bias and absolute error are indicated.

**Fig. 15.** As Fig. 14 but for the upper tropospheric humidity.

*Acknowledgements.* Thanks to F. Chevallier for ECMWF data. Thanks to U. Leiterer and H. Dier from DWD station Lindenberg for their radiosonde data, and to L. Neclos from the Comprehensive Large Array-data Stewardship System (CLASS) of the US National Oceanic and Atmospheric Administration (NOAA) for AMSU data.

Thanks to the ARTS radiative transfer community, many of whom have indirectly contributed by implementing features to the ARTS model.

This study was funded by the German Federal Ministry of Education and Research (BMBF), within the AFO2000 project UTH-MOS, grant 07ATC04. It is a contribution to COST Action 723 “Data Exploitation and Modeling for the Upper Troposphere and Lower Stratosphere”.

Edited by: D. McKenna

## References

- Buehler, S. A. and John, V. O.: A Simple Method to Relate Microwave Radiances to Upper Tropospheric Humidity, *J. Geophys. Res.*, 110, D02110, doi:10.1029/2004JD005111, 2005.
- Buehler, S. A., Kuvatov, M., John, V. O., Leiterer, U., and Dier, H.: Comparison of Microwave Satellite Humidity Data and Radiosonde Profiles: A Case Study, *J. Geophys. Res.*, 109, D13103, doi:10.1029/2004JD004605, 2004.
- Buehler, S. A., Eriksson, P., Kuhn, T., von Engeln, A., and Verdes, C.: ARTS, the Atmospheric Radiative Transfer Simulator, *J. Quant. Spectrosc. Radiat. Transfer*, 91, 65–93, 2005.
- Chevallier, F.: Sampled databases of 60-level atmospheric profiles from the ECMWF analysis, Tech. rep., ECMWF, EUMETSAT SAF program research report no. 4, 2001.
- Elachi, C.: Introduction to the physics and techniques of remote sensing, J. Wiley and Sons, 1987.
- Held, I. M. and Soden, B. J.: Water Vapor Feedback and Global Warming, *Annu. Rev. Energy Environ.*, 25, 441–475, 2000.
- Jimenez, C., Eriksson, P., John, V. O., and Buehler, S. A.: A practical demonstration on AMSU retrieval precision for upper tropospheric humidity by a non-linear multi-channel regression method, *Atmos. Chem. Phys.*, 5, 451–459, 2005, **SRef-ID: 1680-7324/acp/2005-5-451**.
- Leiterer, U., Dier, H., and Naebert, T.: Improvements in Radiosonde Humidity Profiles Using RS80/RS90 Radiosondes of Vaisala, *Beitr. Phys. Atm.*, 70, 319–336, 1997.
- Mo, T.: Prelaunch calibration of the advanced microwave sounding unit-A for NOAA-K, *IEEE Trans. Micr. Theory Techni.*, 44, 1460–1469, 1996.
- Saunders, R. W., Hewison, T. J., Stringer, S. J., and Atkinson, N. C.: The Radiometric Characterization of AMSU-B, *IEEE Trans. Micr. Theory Techni.*, 43, 760–771, 1995.
- Schmetz, J., Menzel, W. P., Velden, C., Wu, X., van de Berg, L., Nieman, S., Heyden, C., Holmund, K., and Geijo, C.: Monthly mean large-scale analyses of upper tropospheric humidity and wind fields derived from three geostationary satellites, *Bull. Am. Meteorol. Soc.*, 76, 1578–1584, 1995.
- Soden, B. J. and Bretherton, F. P.: Upper Tropospheric Relative Humidity From the GOES 6.7  $\mu\text{m}$  Channel: Method and Climatology for July 1987, *J. Geophys. Res.*, 98, 16 669–16 688, 1993.
- Spencer, R. W. and Braswell, W. D.: How Dry is the Tropical Free Troposphere?, Implications for Global Warming Theory, *Bull. Amer. Met. Soc.*, 78, 1097–1106, 1997.
- Udelhofen, P. M. and Hartmann, D. L.: Influence of tropical cloud systems on the relative humidity in the upper troposphere, *J. Geophys. Res.*, 100, 7423–7440, 1995.